# Separation and Determination of Medium Lanthanides: A New Experiment with Use of Ion-Exchange Separation and Fast Fourier Transform Continuous Cyclic Voltammetry

*Mohammad Reza Pourjavid,[1] Parviz Norouzi,[1,2,*] Mohammad Reza Ganjali,[1,2] Ali Nemati,[3] Hassan Ali Zamani,[4] Majid Javaheri[3]*

[1] Center of Excellence in Electrochemistry, Faculty of Chemistry, University of Tehran, Tehran, Iran
[2] Medical Nanotechnology Research Centre, Tehran University of Medical Sciences, Tehran, P.O. Box, 14155-6451, Iran
[3] School of Chemistry, University College of Science, University of Tehran, Tehran, Iran
[4] Department of Applied Chemistry, Quchan branch, Islamic Azad University, Quchan, Iran
[*] E-mail: norouzi@khayam.ut.ac.ir

Separation of medium lanthanides ($Sm^{3+}$, $Eu^{3+}$, $Gd^{3+}$, $Tb^{3+}$ and $Dy^{3+}$) on Nucleosil 100-5-SA (an ion-exchange column) in the presence of α-hydroxyisobutyric acid (HIBA) as an elution agent was investigated. Determinations were performed by Fast Fourier Transform Continuous Cyclic Voltammetry (FFT-CCV) in a flowing solution. It should be stressed that this technique is: simple, precise, accurate, time saving and economical. The influence of HIBA concentration and pH of the eluent was studied. The best performance obtained was at; pH 4.0, scan rate 30 V s$^{-1}$, accumulation potential -300 mV, and accumulation time 0.3 s. The proposed method displays a linear dynamic range between 0.26-23 mg L$^{-1}$ and a detection limit of 0.08 mg L$^{-1}$. Precision, inter-day precision and accuracy of the assay have been presented too. A comparative evaluation of medium lanthanide distribution in sophisticated monazite and xenotime mineral solutions using both FFT-CCV and Inductively Coupled Plasma Atomic Emission Spectrometric (ICP-AES) techniques were carried out. In detail, the advantages this method illustrates in comparison with other reported methods are the following; no necessity for oxygen removal from test solution, a suitable detection limit and fast determination of any such compound in a wide variety of chromatographic methods. Potential waveform consisted of steps for cleaning, accumulation and potential ramp of the analyte, and it was continuously applied on an Au disk microelectrode (12.5 mm in radius).

## 1. INTRODUCTION

Classification and separation of lanthanides is an extremely difficult task because of their: similarity to each other (equal charge and almost similar ionic radii) and presence of them at trace concentration levels in most geological materials [1]. A number of analytical techniques have been reported for the determination of lanthanides in various matrices [2]. Several methods have been reviewed on the utilization of chromatographic and electrophoresis techniques for lanthanide separation and determination [3-15]. These researches explained use of high performance liquid chromatography (HPLC), cation and/or anion exchange chromatography and capillary electrophoresis for separation of lanthanide ions. Detection of them can be found with use of: UV-Vis spectrometry, refractive index (RI) detectors, spectrofluorimetry, ICP-AES and diod array detectors.

As a result of the very similar characteristics of the group elements, the stability constants of metal ions with a particular ligand show only slight differences. Thus, in order to achieve good separation of lanthanides, it is necessary to choose a proper complexing agent. Molecules with structures that are flexible and have rigid coordination could decrease the stability constant of the ligand, but increase the lanthanide(III) ion size selectivity of the ligand due to varied coordination distances and different radii of the ions. Such compounds could provide improved materials for the separation of these ions [16].

Use of ion chromatography for lanthanide analysis is an attractive procedure. In this method, typically, stationary phases are low-capacity cation-exchange resins with aqueous solutions of complexing agents as mobile phases. The most useful eluents for separation of lanthanides are α-hydroxyisobutyricacid (α -HIBA) [17,18], mandelic acid [19], oxalic acid [20], glycolic acid [21], and lactic acid [22]. Recently, Fernández and Alonso used ethylendiaminetetraacetic acid as a mobile phase for lanthanide separation [23]. A mixed gradient of two eluents can sometimes be used for lanthanide separations [24]. The most popular eluting agent amongst different hydroxycarboxylic acids is HIBA. It can provide a good degree of separation between adjacent lanthanides in ion chromatography. Lanthanide ions and HIBA form positive complexes with a single charge that lowers the affinity of the lanthanide for the cation-exchange resin. Reducing the charge of lanthanides (in complex form) causes a reduction in their retention on the stationary phase. The difference in stability constants for the lanthanide-HIBA complex implies that each lanthanide will spend more or less time in the eluent depending on its relative stability with HIBA. Increasing the atomic number of elements increases the degree of complexation and its effect on the resulting charge of the complex. Therefore, lanthanides that form the most stable complex with HIBA such as dysprosium will spend relatively more time in the eluent and elute first. Lanthanides such as samarium form a weaker complex with HIBA and spend relatively less time in the eluent. These metal ions spend more time in the resin and elute later. The use of stronger complexing agents such as oxalic acid results in the formation of anionic lanthanide ions. Under these conditions, the lanthanide series may be separated by anion-exchange. Because the strongest complexes are the most negatively charged, the elution order is reversed from that of the cation-exchange separations. So, in this paper we used HIBA as an eluting agent.

Traditionally, lanthanides are detected by post-column spectrophotometric reaction with strongly absorbing chromophores such as PAR or Arsenazo-III [3,25]. Recently the separated lanthanides have been most commonly determined using ICP-AES and ICP-MS as an ion chromatography interface [26,27]. However, a serious problem in this case is a large amount of reagent is used as the mobile phase, and thus may cause spectral interferences duo to molecular bands such as CO, CN, OH or NH. Also, due to the high viscosity of concentrated salt solutions, they tend to influence the nebulization efficiency. In the case of ICP-MS, polyatomic ions cause major interferences.

Potentiometric sensors can offer an inexpensive and convenient analysis method of rare-earth ions in solution provided that acceptable sensitivity and selectivity are achieved. There are many reports about ion selective electrodes (ISEs) for lanthanide ions in last decade [28-35]. The aim of the present study is determination of samarium, europium, gadolinium, terbium and dysprosium by Fast Fourier Transform Continuous Cyclic Voltammetry (FFT-CCV). Detection of lanthanide ions with FFT-CCV is faster than other detection methods, especially UV-Vis spectrometry, because in these methods pre- or post- column derivatization is necessary which can be time consuming and expensive.

Applying the stripping voltammetric technique in flowing solutions allows movement of the analyte zone in an electrochemical flow cell, resulting in fast accumulation of the analyte and fast potential sweeping (which is not appropriate for large electrodes) [36]. In the case of irreversible systems, electrochemical measurements at solid electrodes are not suitable. This is because the easy deactivation (or poisoning) of the surfaces of the solid electrodes by products of the red/ox reactions of the desired species or impurities is present in the solution. However, most of the problems of such methods can be overcome by the application of ultra-microelectrodes (UMEs). The application of voltammetric techniques has been further stimulated by the advent of UMEs, e.g. their steady state currents, higher sensitivity due to increased mass transport, and their ability to be used in solutions with a very high resistance [37]. UMEs have been applied as sensors in various techniques like: Flow Injection Analysis (FIA) [38], cardiovascular monitoring and in the analysis of some organic compounds [39]. Another problem comes from the changes in the characteristics of the electrode surface during the potential scan. The electrode signal will have a large background current if the surface of the solid electrode is oxidized and reduced during voltammetric measurements (the response of the electrode will have a large background current), which is associated with high levels of noise due to the structural changes of the electrode surface. Currents like this can interfere with the electrode processes of interest and may adversely affect the detection limits of the methods used.

The background current in voltammetric measurements can provide useful information about the adsorption processes and changes in the double layer at the electrode surface [40]. In addition, small amounts of adsorption of species present in the solution on the electrode surface can strongly affect the cathodic and anodic currents of red/ox reactions of the electrode. For calculation of the signal of the analyte and noise reduction, a special computer based numerical method can be introduced. The calculation of signal was based on the net partial and total charge exchanges at the electrode surface and was done by integrating the currents at the selected potential range at the cyclic voltammogram (CV). Depending on the conditions applied the detector can be used in determination of various species in chromatographic analysis methods (e.g. HPLC and IC).

## 2. EXPERIMENTAL PART

### 2.1. Apparatus

The model IC760 (Metrohm) was used during ion chromatographic experiments. Characterization of some useful cation exchangers was presented in Table 1 [41]. However, in the case of separation of the medium lanthanides the ion-exchanger DOWEX 50WX8 was used. The operation was completed under the flow rate 1.5 mL min$^{-1}$.

The equipment for flow injection analysis included a 10 roller peristaltic pump (UltrateckLabs Co., Iran) and a four-way injection valve (Supelco Rheodyne Model 5020) with a 50 μL sample injection loop. Solutions were introduced in the sample loop by means of a plastic syringe. After opening the loop in the way of eluent flow, the sample passed over the working electrode. The electrochemical cell used in flow-injection analysis is shown in Fig. 1. The potentiostate applied a potential in the range of gold oxidation in acidic media and the potential waveform is shown in Fig 2. The volume of the cell was 100 μL. In all experiments described in this paper, the flow rate of eluent solution was 3 mL min$^{-1}$.

A Varian Liberty 150 AX Turbo model inductively coupled plasma-Atomic Emission spectroscopy (ICP-AES) was used for the determination of the lanthanide ion concentration. latinum.

**Table 1.** Characterization of cation-exchanger

| Character (*) | Trade Name | Procedure (**) | Active Group | Matrix | Effective pH | Total Exchange Capacity (meq/ml) | Standard Mesh Range |
|---|---|---|---|---|---|---|---|
| SAC | Dowex 50 | 1 | Sulfonic acid | Polystyrene | 0-14 | Na$^+$ 1.9 H$^+$ 1.7 | 20-50 (wet) |
| SAC | Dowex MPC-1 | 4 | Sulfonic acid | Polystyrene | 0-14 | 1.6-1.8 H$^+$ form | 20-40 (wet) |
| SAC | Dowex 50WX8 | 1 | Sulfonic acid | Polystyrene | 0-14 | 1.7 H$^+$ form | 50-100 |
| SAC | Duolite C-20 | 2 | Sulfonic acid | Polystyrene | 0-14 | 2.2 | 16-50 |
| SAC | Ionac 240 | 3 | Sulfonic acid | Polystyrene | 0-14 | 1.9 | 16-50 |
| SAC | Duolite C-3 | 2 | Methylene Sulfonic | Phenolic | 0-9 | 1.1 | 16-50 |
| WAC | Dowex CCR-1 | 4 | Carboxylic | Phenolic | 0-9 | - | 20-50 (wet) |
| WAC | Duolite ES-63 | 2 | Phosphonic | Polystyrene | 4-14 | 3.3 | 16-50 |
| WAC | Duolite ES-80 | 2 | Aliphatic | Acrylic | 6-14 | 3.5 | 16-50 |

\* SAC: Strong Acid Cation, WAC: Weak Acid Cation
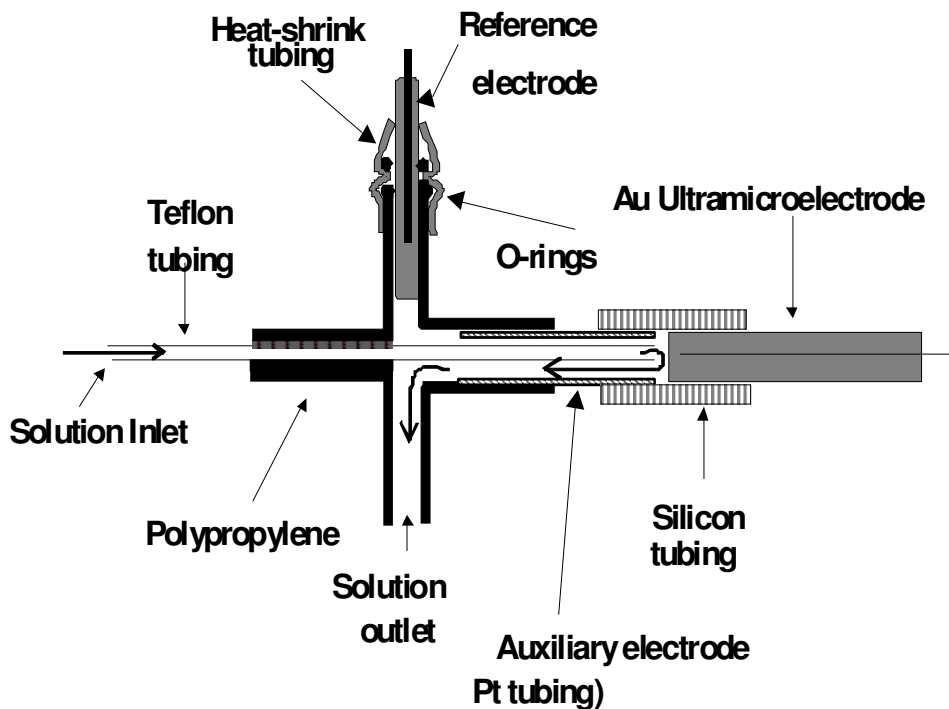\*\* 1. Dow, 2. Diamond Shamarck, 3. Ionac, 4. Nalco

**Figure 1.** Diagram of the electrochemical cell

## 2.2. Reagents

For the experimental part of this research the oxide of lanthanides, hydrochloric acid and HIBA were of high purity available from Merck Chemicals and were used without further purification. HIBA 0.25 mol $L^{-1}$ was buffered at pH 4.0 with sodium hydroxide. The reagents for the preparation of the eluent solution for flow injection analysis (0.05 mol $L^{-1}$ $H_3PO_4$) and 1 mol $L^{-1}$ NaOH (for the pH eluent adjustment), were obtained from Merck. All solutions were prepared in doubly distilled deionized water, filled with the background electrolyte solution and they were used without the removal of dissolved oxygen.

## 2.3. Background electrolyte (BGE) and standard solutions

The running buffer (BGE) was made by the addition of 8.7 mL of phosphoric acid (85% w/v) into a 1000 mL volumetric flask and diluted to a constant volume with distilled water. The pH was adjusted to 4.0 with sodium hydroxide and all solutions were freshly prepared and filtered using a Millipore filter (0.45 μm) each day.

A standard stock solution of lanthanides was prepared in distilled water by dissolving pure lanthanide oxides in 0.36 mol $L^{-1}$ hydrochloric acid. These lanthanide solutions were diluted with doubly distilled deionized water to about 10 mg $L^{-1}$ of metal in standard solutions. Aliquots of standard stock solution of lanthanides were dispensed into 10 mL volumetric flasks and the flasks made up to volume with the running buffer to give final concentrations ranging between 0.01 – 23 mg $L^{-1}$.

*2.4. Electrode preparation*

Gold UMEs (12.5 μm in diameter) were prepared by sealing metal micro-wires (Good fellow Metals Ltd., UK) into a soft glass capillary. The capillary was cut perpendicular to its length to expose the wire. Electrical contacts were made using silver epoxy (Johnson Matthey Ltd., UK). Before each experiment, the electrode surface was polished for 1 min using extra fine carborundum paper and then for 10 min with 0.3 μm alumina. Prior to being placed in the cell the electrode was washed with water. In all measurements, an Ag(s)| AgCl(s)| KCl (aq, 1 mol L$^{-1}$) reference electrode was used. The auxiliary electrode was made of a Pt wire, 1 cm length and 0.5 mm in diameter.

## 3. RESULTS AND DISCUSSION

*3.1. Data acquisition and processing*

For the data acquisition a setup of a PC PIV Pentium 900 MHz microcomputer equipped with a data acquisition board (PCL-818HG, Advantech. Co.), and a custom made potentiostat was used. All data acquisition and data processing programs were developed in Delphi 6$^{®}$ program environment. In Fig. 2, the hypothetical applied waveform potential diagram during the cyclic voltammetric measurements is shown. The potential waveform consists of three parts; (a) potential steps, $E_{c1}$ and $E_{c2}$ (which are used for oxidation and reduction of the electrode surface, respectively), during which the electrochemical cleaning of the electrode surface takes place, (b) $E_c$, where the analyte accumulation takes place, and (c) the potential ramp where the current measurements occur.
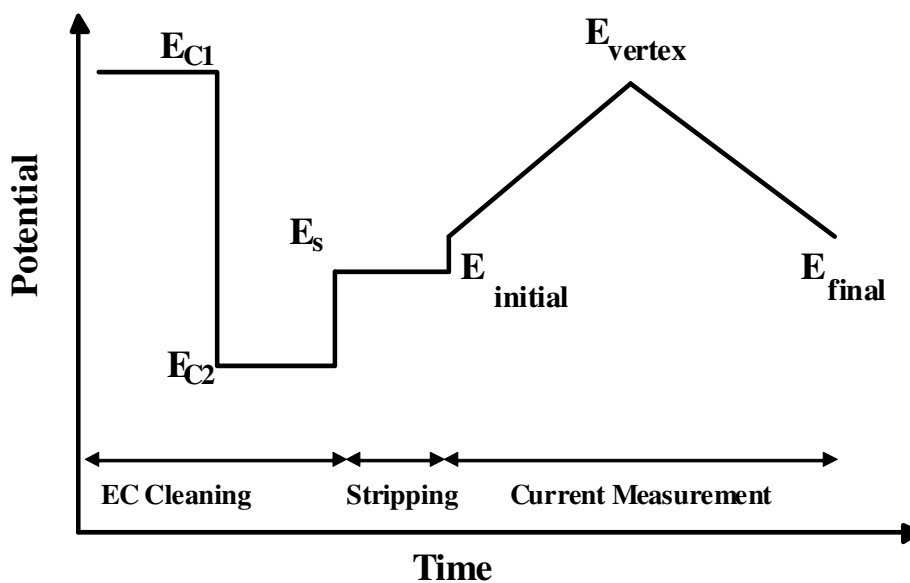


**Figure 2.** The diagram of the applied potential waveform

During the scan some of the adsorbed analyte molecules are desorbed. Depending on the rate of those processes and the scan rate, the amount of the desorption analyte molecules (during the scan) can be changed. An important point to note is that: some of the adsorbed analyte molecules remain on the electrode surface inhibiting the red/ox process of the electrode surface. In this technique, *ΔQ* is calculated according with all current changes at the CVs [42-46].

One of the considerable aspects of this method is the application of a special digital filtration that is applied during the measurement. At first, an electrode CV was recorded and then by applying FFT on the collected data, the existing high frequency noises were determined. With the aid of this information the cutoff frequency of the analog filter was set at a certain value (where the noises were removed from the CV).

Since the crystal structure of a polycrystalline gold electrode is greatly affected by the condition of the applied potential waveform [37], different potential waveforms were examined in order to obtain a reproducible electrode surface (or a stable background signal). In fact, the application of cyclic voltammetry for the determination of electroactive compounds mainly faces low stability of the background signal due to the changes taking place on the surface crystal structure during the oxidation and reduction of the electrode in each potential cycle.

The electrochemical oxidation process on the gold surface starts with the hydroxyl ion electrosorption, which at more positive potentials results in the gold oxide formation undergoing structural rearrangement [47].
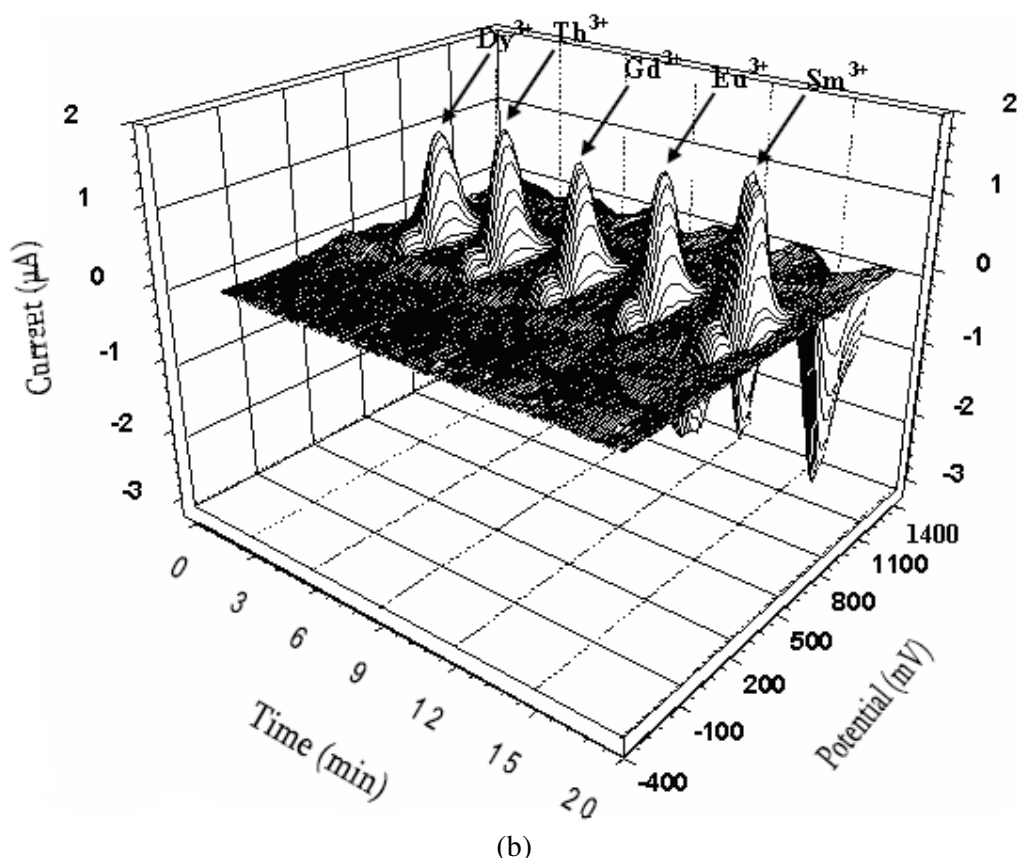


(a)

(b)
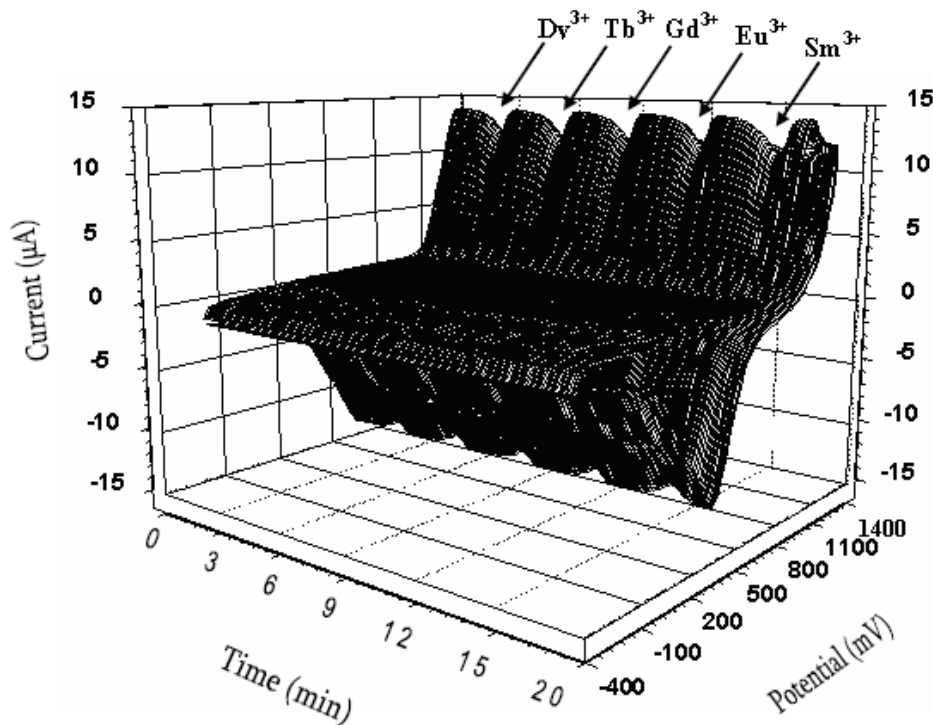
**Figure 3.** (a) Cyclic voltammogram at a 12.5 µm Au ultramicroelectrode recorded during a flow injection experiment. The eluent was 0.05 mol L$^{-1}$ H$_3$PO$_4$, the flow rate was 100 µL s$^{-1}$ and the sweep rate was 30 V s$^{-1}$. Each scan was preceded by 100 ms (at 600 mV) and 100 ms (at -800 mV) conditioning, respectively. The accumulation time was 300 ms at -300 mV. The injected solution (50 µL) contained 1.0 mg L$^{-1}$ Sm$^{3+}$, Eu$^{3+}$, Gd$^{3+}$, Tb$^{3+}$ and Dy$^{3+}$ in 0.05 mol L$^{-1}$ H$_3$PO$_4$. (b) Curves result from the subtraction of the CVs average (in the absence of the analytes) from the test of the CVs in (a).

An example of the recorded CVs is demonstrated in Fig. 3 (a and b). Figure 3a shows a CV sequence recorded during the flow analysis for the lanthanides determination. The injection volume was 50 µL of (1.0 mg L$^{-1}$) Sm$^{3+}$, Eu$^{3+}$, Gd$^{3+}$, Tb$^{3+}$ and Dy$^{3+}$ (in 0.05 mol L$^{-1}$ H$_3$PO$_4$) into the eluent solution, containing 0.05 mol L$^{-1}$ H$_3$PO$_4$. The time axis of the graph represents the time of the flow injection experiment. In the absence of medium lanthanide ions, the shape of the CV curve is typical for a polycrystalline gold electrode in acidic media [48]. Figure 3b illustrates the absolute current changes in the CV curves, after subtracting the average background of 4 CVs (in the absence of the analytes). Evidently, this way of presenting the electrode response gives more details about the adsorbed ion effect on the CV currents. As a matter of fact, the curves show that the current changes mainly take place at the potential regions of the oxidation and reduction of gold. When the electrode-solution interface is exposed to medium lanthanide ions, which can be adsorbed on the electrode, the oxide formation process becomes severely inhibited. In detail, the surface process inhibition causes significant change in the currents at the potential region and, as a consequence, the profound changes in the shape of the CVs take place.

Theoretically, the analyte response can be affected by the thermodynamic and kinetic parameters of adsorption, the mass transport rate and the electrochemical behavior of the adsorbed species. The free energy and the adsorption rate depend on the electrode potential, the electrode material and, to some extent, on the choice of the concentration and the type of the supporting electrolyte. By taking these points into consideration for the achievement of the detector maximum performance, the effect of the experimental parameters (such as pH of the supporting electrolyte, potential, accumulation time and potential scan rate) must be examined and optimized [47-52].

*3.2. Experimental parameter optimization*

Stability constants of the Ln-eluent complexes affect the elution pattern of lanthanides. If the stability constant of Ln-eluent complexes increases, its elution will be faster. The lesser the stability constant of complex, the slower the elution will be. Generally for all the eluents the stability constant increases from Sm to Dy and this explains the elution pattern in the order of decreasing atomic number from Dy to Sm in the cation-exchanger. The nature of the metal ion and eluent as well as the environmental factors such as solvent/medium, concentration, temperature and pressure can affect the formation of a complex between them. Hence, the stability constants for a given metal-eluent complex under different environmental conditions can be different. The log values of the stability constant for complexes of light lanthanides with HIBA vary from 6.77 for Sm(III) to 7.87 for Dy(III), and correspond to the reported literature [53] given in Table 2. These give a qualitative picture of the behavior during separation of lanthanides; however the exact performance can be different.

**Table 2.** Stability constants ($\log K$) of medium lanthanides with α-HIBA used as complexing agent at 20°C

| Lanthanide | $\log K$ |
|------------|----------|
| Samarium | 6.77 |
| Europium | 7.32 |
| Gadolinium | 7.19 |
| Terbium | 7.43 |
| Dysprosium | 7.87 |

*3.3. Effect of pH of eluent on retention of lanthanide ions*

Effect of the mobile phase pH on the elution pattern of a mixture of light lanthanide ions using HIBA is shown in Fig. 4. This effect was monitored using the retention factor ($K$). The analytical expression for $K$ is:

$$K = \frac{(t_R - t_0)}{t_0} \qquad (1)$$

In this equation $t_0$ is retention time of the non-retained peak, and $t_R$ is retention time of the eluent retained. Increasing the pH from 3.0 to 6.0 caused a decrease in retention factor ($K$) for lanthanide ions. The elution efficiency of carboxylic acids changes with pH - this factor depends on the strength of carboxylic acid, which depends on its pH. The α-hydroxycarboxylic acids tested were weak and undergo only partial ionization and show poor eluting strength at low pH [14]. With increasing pH, the elution efficiency increased due to greater ionization of the –COOH group. At higher pH, the retention factors for different lanthanides are quite close. So, pH 4.0 was selected as the optimum providing adequate resolution in a shorter time. Furthermore this pH was chosen because it is near to that of the maximum buffer capacity for HIBA.
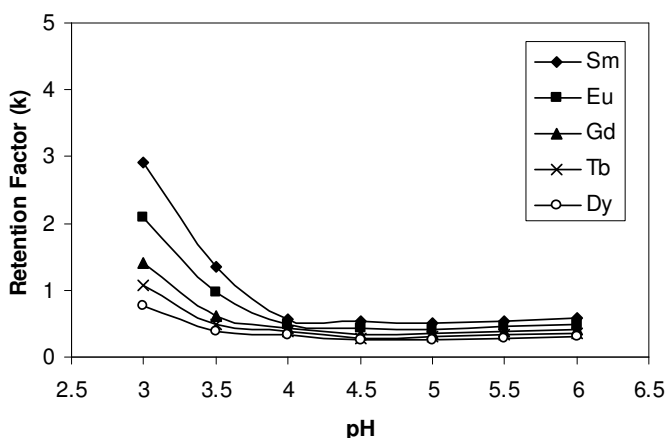


**Figure 4.** Effect of pH of mobile phase on retention of light lanthanides DOWEX 50WX8 under isocratic condition: 0.25 mol $L^{-1}$ of HIBA. The injected solution (50 µL) contained 1.0 mg $L^{-1}$ $Sm^{3+}$, $Eu^{3+}$, $Gd^{3+}$, $Tb^{3+}$ and $Dy^{3+}$ in 0.05 mol $L^{-1}$ $H_3PO_4$.



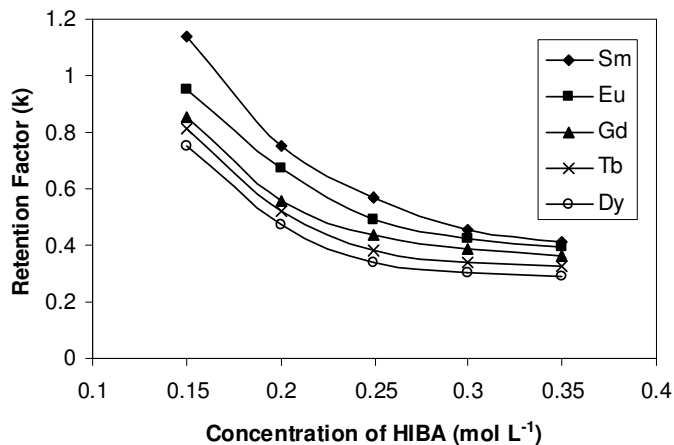**Figure 5.** Effect of concentration of HIBA, pH 4.0 on retention of lanthanides on DOWEX 50WX8. The injected solution (50 µL) contained 1.0 mg $L^{-1}$ $Sm^{3+}$, $Eu^{3+}$, $Gd^{3+}$, $Tb^{3+}$ and $Dy^{3+}$ in 0.05 mol $L^{-1}$ $H_3PO_4$.

*3.4. Effect of concentration of eluent on retention of lanthanide ions*

The influence of the concentration of HIBA on retention of medium lanthanides is shown in Fig. 5. In high concentrations of eluent elution of lanthanides is faster. The effect of concentration of HIBA was studied at pH 4.0. Under this condition HIBA is ~ 63% ionized ($pK_a = 3.77$) [54]. With the increase in concentration of α-HIBA the concentration of α-hydroxyisobutyrate ions increases in the mobile phase and results in faster elution of lanthanides on the column.
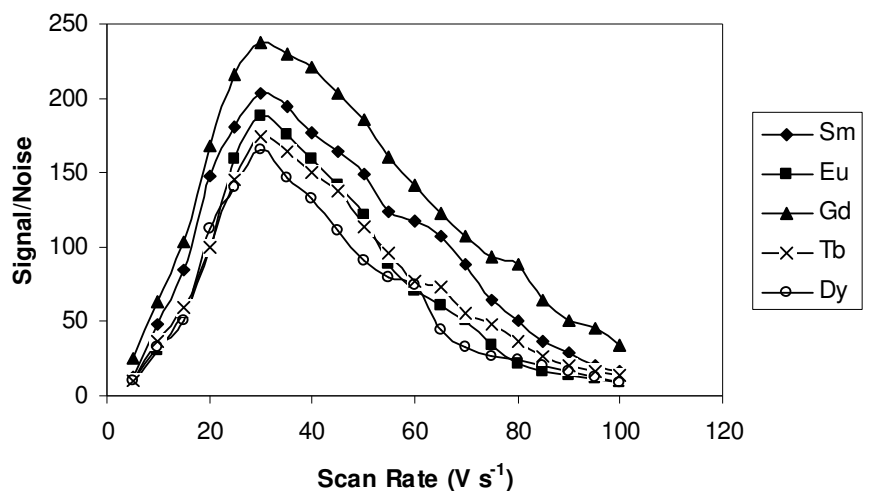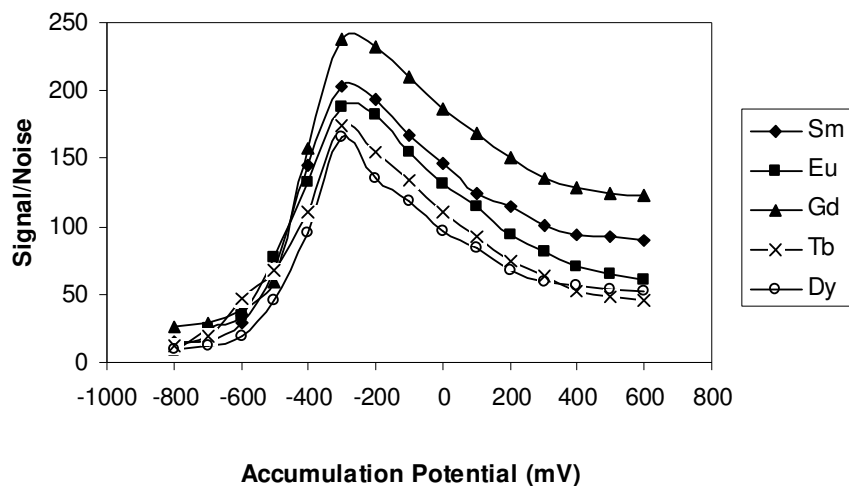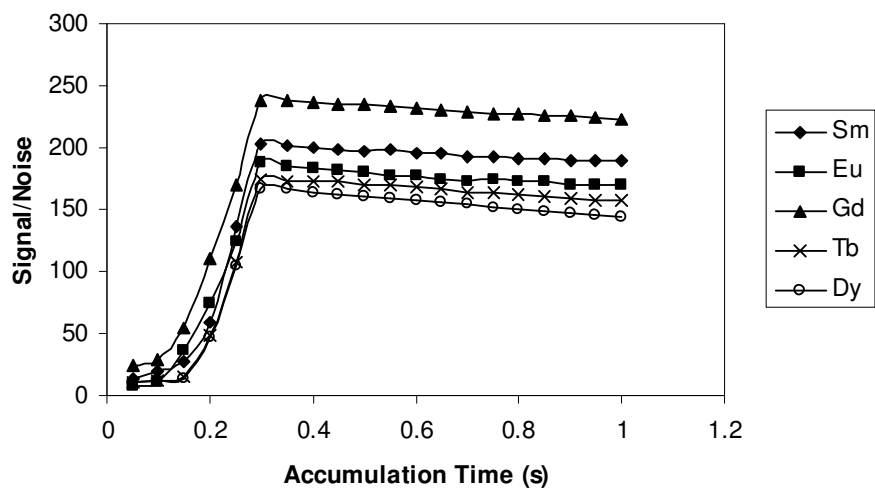
(a)
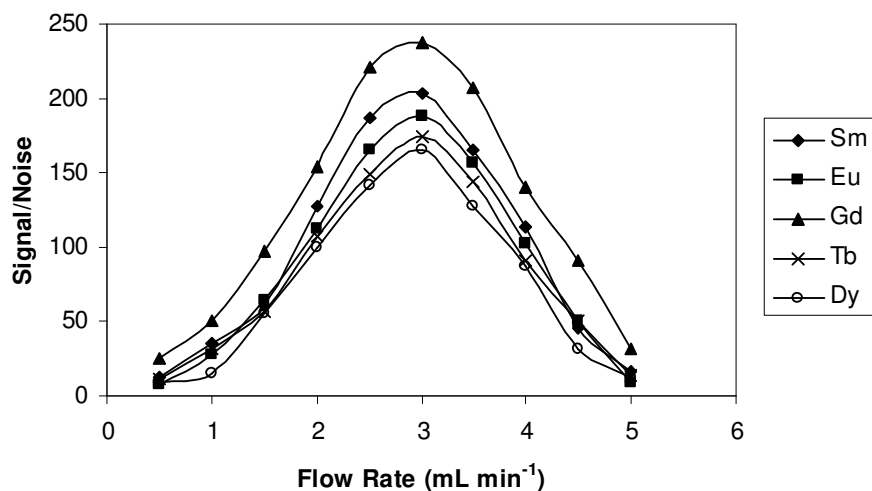
(b)

**Figure 6.** (a) The effect of the sweep rate and (b) the effect of flow rate on the response of the Au electrode (with a radius of 12.5 µm) to injections of 1.0 mg L$^{-1}$ Sm$^{3+}$, Eu$^{3+}$, Gd$^{3+}$, Tb$^{3+}$ and Dy$^{3+}$ in 0.05 mol L$^{-1}$ H$_3$PO$_4$.

(a)



(b)

**Figure 7.** (a) The effect of the accumulation potential and (b) the effect of the accumulation time on the electrode response to injections of 1.0 mg L$^{-1}$ Sm$^{3+}$, Eu$^{3+}$, Gd$^{3+}$, Tb$^{3+}$ and Dy$^{3+}$ in 0.05 mol L$^{-1}$ H$_3$PO$_4$.

*3.5. Influence of sweep rate, accumulation potential and accumulation time*

For the investigation of the scan rates influence and eluent flow rate on the sensitivity of detector response, solutions having a concentration of 1.0 mg L$^{-1}$ in Sm$^{3+}$, Eu$^{3+}$, Gd$^{3+}$, Tb$^{3+}$ and Dy$^{3+}$ were injected. At different scan rates (from 5 to 100 V s$^{-1}$) and eluent flow the detector responses to the injected sample were recorded. These results are presented in Fig. 6. As it is clear from Fig. 6a the detector exhibits the maximum sensitivity at a scan rate of 30 V s$^{-1}$, and Fig. 6b shows that flow rate of 3 mL min$^{-1}$ is the best. The sweep rate affects the detection performance and can be considered in three

different aspects: (a) speed in data acquisition, (b) kinetic factors of lanthanide ions adsorption and, (c) eluent flow rate which controls the time window of the solution zone in the detector. The main reason for application of high scan rates is prevention from desorption of the adsorbed lanthanide ions during the potential scanning (because under this condition, the inhibition outcome of the adsorbed lanthanide ions on the oxidation process can take place).

It is a fact that the employment of high scan rates is required for the use of this detection method in conjunction with fast separation techniques, such as capillary electrophoresis. From this point of view it is necessary to check how the method sensitivity is affected by the sweep rate. Therefore, high sweep rates must be employed to detect the amount of adsorbed analyte on the electrode surface so that the potential scanning step is short in comparison with the accumulation period. An important point to be taken into consideration is the time when the lanthanide ion accumulation occurs at a potential that is greater or smaller than $E_i$. However, the sensitivity of the detection system mainly depends on the potential sweep rate mostly because of the adsorption kinetic factors and the instrumental limitations. Notably, any changes in the parameters related to the adsorption process affecting the applied potential, the time and the potential of accumulation severely influences the sensitivity of the measurement. For that reason the influence of the accumulation potential and time on the response of the method for the injection of a solution of (1.0 mg $L^{-1}$) $Sm^{3+}$, $Eu^{3+}$, $Gd^{3+}$, $Tb^{3+}$ and $Dy^{3+}$ in 0.05 mol $L^{-1}$ $H_3PO_4$ was studied. Figure 7 shows the detector response over the accumulation potential ranges from −800 to 600 mV and the accumulation time range from 0.05 to 1.0 s. Figure 7a and 7b derives the conclusion that the optimum conditions to be chosen are accumulation potential of -300 mV and accumulation time of 300 ms, on the grounds that the electrode surface becomes lanthanide ions saturated within a (1300 ms) time window.

On the electrode the lanthanide ions accumulation takes place during the accumulation step (assuming that an appropriate potential is selected). The difference in the saturation time of the various compounds can be related to the existing differences in their kinetics of the electron transfer and mass transport. As mentioned above, the surface of the gold ultra microelectrode is small and in a short time the electrode surface can be saturated.

*3.6. Validation*

The method was validated in terms of: linearity, limit of quantitation (LOQ), limit of detection (LOD), precision, accuracy, ruggedness/robustness, recovery and selectivity.

The linearity was evaluated by linear regression analysis, which was calculated by the least square regression method. The calibration curves constructed for medium lanthanide ions were linear over the concentration range of 0.26–23 mg $L^{-1}$. The peak areas of $Sm^{3+}$, $Eu^{3+}$, $Gd^{3+}$, $Tb^{3+}$ and $Dy^{3+}$ were plotted versus its concentration and linear regression analysis was carried out on the resultant curve. After this analysis a correlation coefficient of $R = 0.999$ and %R.S.D. values ranging from 0.16 to 3.3% across the studied concentration range were obtained. Typically, the regression equation for the calibration curve was found to be Y=3.3942X+151.58, Y=2.0081X+38.867, Y=3.7313X+243.72, Y=3.0985X+66.052 and Y=3.0306X+15.629 for $Sm^{3+}$, $Eu^{3+}$, $Gd^{3+}$, $Tb^{3+}$ and $Dy^{3+}$ respectively. Figure
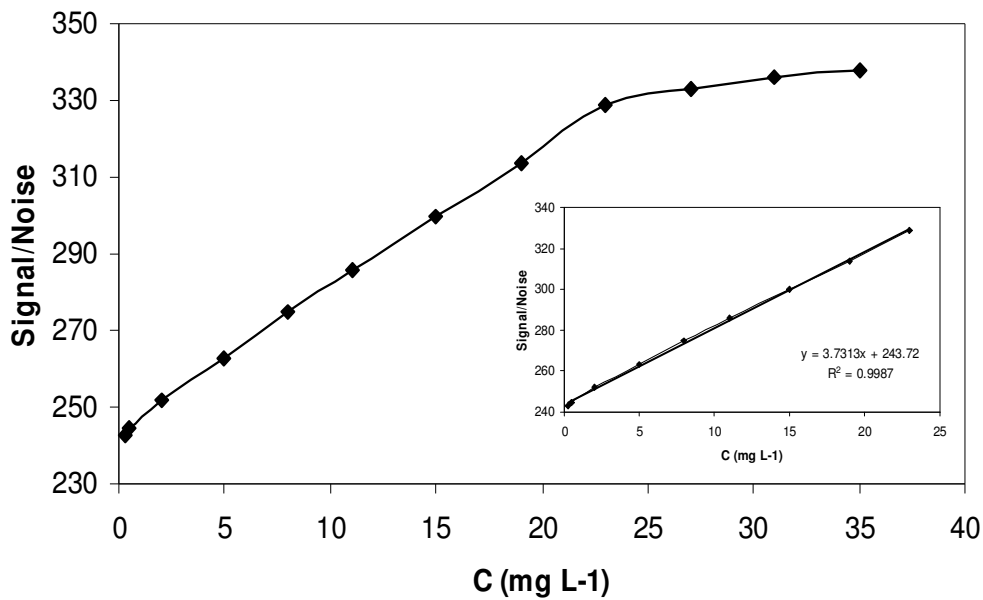
8 depicts the calibration graph that resulted from the monitoring of these lanthanide ions in a 0.05 mol L$^{-1}$ H$_3$PO$_4$.
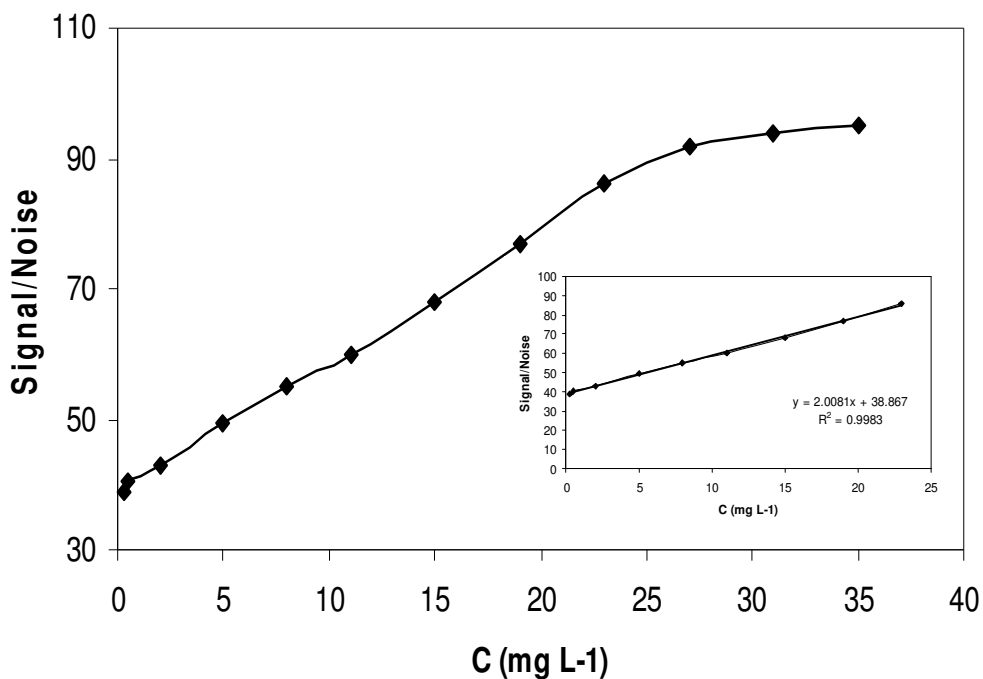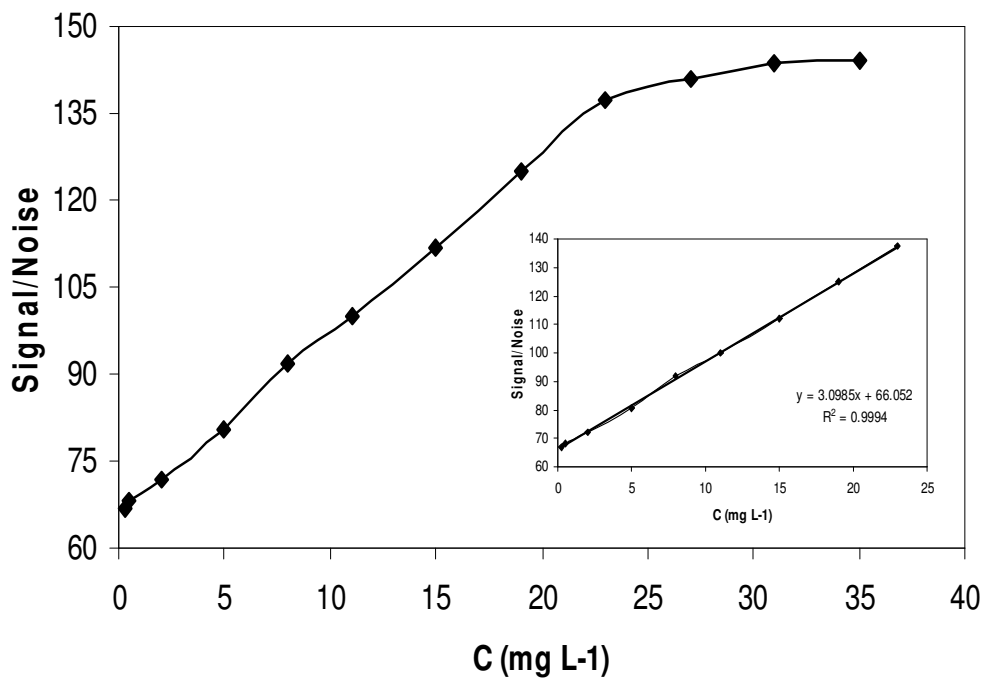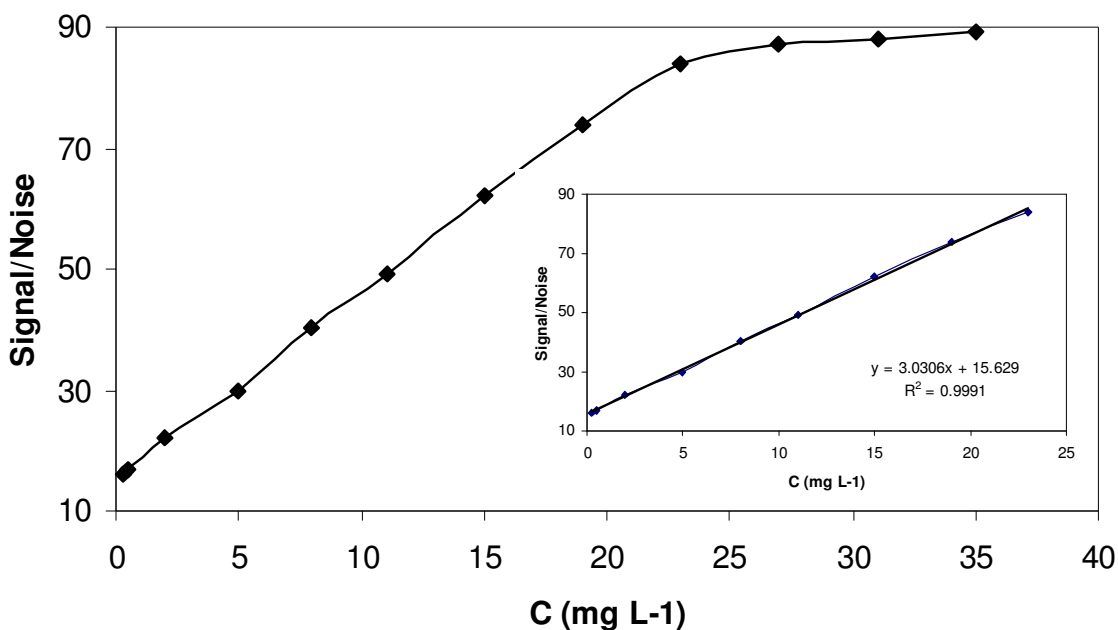


(a)
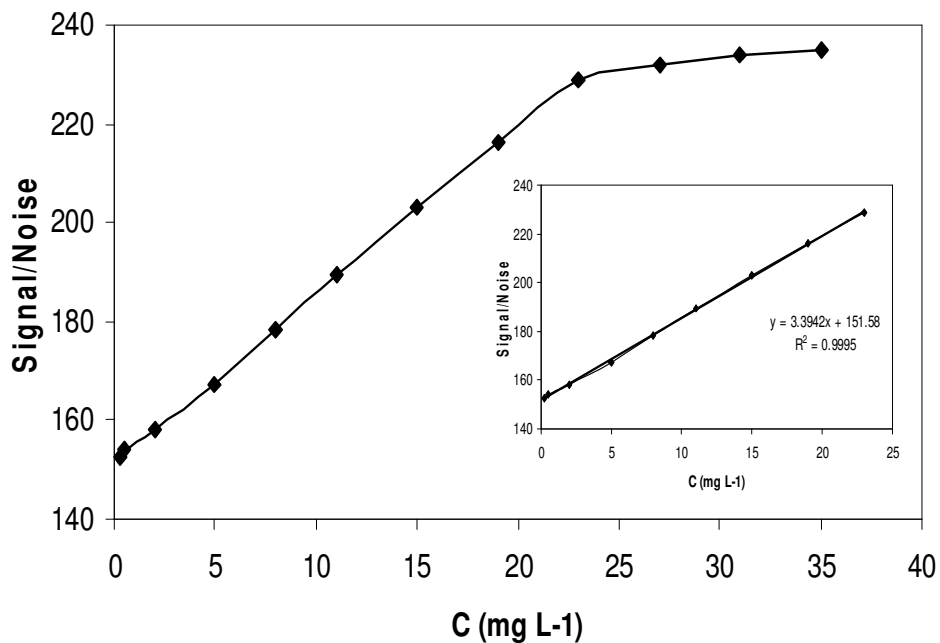


(b)

(c)



(d)

(e)

**Figure 8.** Calibration curves obtained for (a) $Sm^{3+}$, (b) $Eu^{3+}$, (c) $Gd^{3+}$, (d) $Tb^{3+}$, (e) $Dy^{3+}$ ions on the Au electrode in 0.05 mol $L^{-1}$ $H_3PO_4$ under isocratic condition: 0.25 mol $L^{-1}$ of HIBA, Scan rate: 30 V $s^{-1}$, Flow rate: 3 mL $min^{-1}$.

Concerning the LOD value, it was measured as the lowest analyte amount that may be detected to produce a response that is significantly different from that of a blank one. The limit of detection was approved by calculations based on the standard deviation of the response ($\delta$) and the slope ($S$) of the calibration curve at the levels approaching the limits according to the equation LOD=3.3 ($\delta/S$) [55]. The LOD for $Sm^{3+}$, $Eu^{3+}$, $Gd^{3+}$, $Tb^{3+}$ and $Dy^{3+}$ was found to be 0.08 mg $L^{-1}$. On the other hand, the LOQ was measured as the lowest analyte amount that can be reproducibly quantified above the baseline noise for which triplicate injections resulted in an R.S.D. ≤1.3 %. A practical LOQ giving good precision and acceptable accuracy was equivalent to 0.26 mg $L^{-1}$.

The precision of the assay was investigated with respect to both repeatability and reproducibility. The repeatability was investigated by injecting nine replicate samples of each of the (0.26, 15 and 23 mg $L^{-1}$) standards. Additionally, injecting the same three concentrations over three consecutive days allowed the inter-day precision to be assessed. The results are shown in Table 3.

**Table 3.** Precision and inter-day precision of the assay

| | Standard Solutions(mg L$^{-1}$) | Precision | | Inter-day Precision | |
|---|---|---|---|---|---|
| | | Mean Concentration (mg L$^{-1}$) | RSD (%) | Mean Concentration (mg L$^{-1}$) | RSD (%) |
| Sm$^{3+}$ | 0.26 | 0.26 | 0.03 | 0.27 | 0.04 |
| | 15 | 15.02 | 0.03 | 15.03 | 0.04 |
| | 23 | 22.88 | 0.01 | 22.87 | 0.02 |
| Eu$^{3+}$ | 0.26 | 0.26 | 0.04 | 0.27 | 0.05 |
| | 15 | 15.03 | 0.03 | 15.04 | 0.03 |
| | 23 | 22.87 | 0.02 | 22.87 | 0.03 |
| Gd$^{3+}$ | 0.26 | 0.26 | 0.03 | 0.28 | 0.04 |
| | 15 | 15.04 | 0.02 | 15.05 | 0.04 |
| | 23 | 22.88 | 0.01 | 22.87 | 0.02 |
| Tb$^{3+}$ | 0.26 | 0.27 | 0.04 | 0.27 | 0.04 |
| | 15 | 15.03 | 0.02 | 15.04 | 0.03 |
| | 23 | 22.97 | 0.02 | 22.06 | 0.02 |
| Dy$^{3+}$ | 0.26 | 0.27 | 0.04 | 0.28 | 0.05 |
| | 15 | 15.05 | 0.02 | 15.05 | 0.03 |
| | 23 | 22.05 | 0.01 | 22.05 | 0.02 |

**Table 4.** Accuracy of the assay

| | Standard Solutions (mg L$^{-1}$) | Resultant Concentration (mg L$^{-1}$) | Relevant Error (%) |
|---|---|---|---|
| Sm$^{3+}$ | 0.26 | 0.27 ± 0.03 | 3.85 |
| | 15 | 15.03 ± 0.22 | 0.20 |
| | 23 | 22.90 ± 0.49 | 0.04 |
| Eu$^{3+}$ | 0.26 | 0.27 ± 0.02 | 3.85 |
| | 15 | 15.10 ± 0.40 | 0.67 |
| | 23 | 22.91 ± 0.25 | 0.39 |
| Gd$^{3+}$ | 0.26 | 0.26 ± 0.05 | 1.92 |
| | 15 | 15.09 ± 0.12 | 0.60 |
| | 23 | 22.89 ± 0.39 | 0.48 |
| Tb$^{3+}$ | 0.26 | 0.27 ± 0.03 | 3.85 |
| | 15 | 15.08 ± 0.50 | 0.53 |
| | 23 | 22.85 ± 0.11 | 0.65 |
| Dy$^{3+}$ | 0.26 | 0.26 ± 0.04 | 1.54 |
| | 15 | 15.11 ± 0.26 | 0.73 |
| | 23 | 22.91 ± 0.18 | 0.39 |

The accuracy of the assay was determined by the interpolation of replicate (*n*=6) peak areas of three accuracy standards (0.26, 15 and 23 mg L$^{-1}$) from a calibration curve prepared as previously

described. In each case the relevant error percentage and the accuracy were calculated. Table 4 shows the resultant concentrations with their relevant error percentage.

**Table 5.** Influence of the changes in the experimental conditions on the performance of the FIA system

| Parameter | Modification | %Recovery | | | | |
|---|---|---|---|---|---|---|
| | | $Sm^{3+}$ | $Eu^{3+}$ | $Gd^{3+}$ | $Tb^{3+}$ | $Dy^{3+}$ |
| pH | 3.9 | 98.8 | 100.3 | 100.6 | 101.4 | 98.7 |
| | 4.0 | 100.0 | 101.5 | 1008 | 100.9 | 100.0 |
| | 4.1 | 100.1 | 99.6 | 100.4 | 100.4 | 99.4 |
| Flow Rate | 2.6 | 100.2 | 98.7 | 100.4 | 100.6 | 99.3 |
| (mL/min) | 2.8 | 101.2 | 99.8 | 101.1 | 101.0 | 100.8 |
| | 3.0 | 100.0 | 100.1 | 99.2 | 100.6 | 98.7 |
| Buffer | 0.25 | 101.1 | 100.4 | 100.4 | 99.7 | 100.6 |
| Composition | 0.24 | 101.1 | 100.8 | 99.9 | 100.1 | 100.3 |
| (M) | 0.23 | 99.8 | 100.2 | 100.0 | 98.7 | 100.3 |
| Lab. | 20 | 100.3 | 98.6 | 100.6 | 99.2 | 101.2 |
| Temprature | 25 | 100.6 | 100.1 | 100.7 | 99.8 | 100.9 |
| (°C) | 30 | 100.1 | 99.7 | 100.6 | 99.8 | 100.4 |

**Table 6.** Comparison between the determination of medium lanthanide ions by FFT-CCV and ICP-AES

| Element | Real Amount of Monazite Solution (mg $L^{-1}$) | Found Amount of Monazite Solution (mg $L^{-1}$) | | Real Amount of Xenotime Solution (mg $L^{-1}$) | Found Amount of Xenotime Solution (mg $L^{-1}$) | |
|---|---|---|---|---|---|---|
| | | FFT-CCV | ICP-AES | | FFT-CCV | ICP-AES |
| Sm | 3.00 | 3.44±0.22 | 3.39±0.22 | 19.00 | 20.33±0.14 | 20.57±0.35 |
| Eu | 1.00 | 1.18±0.12 | 1.18±0.12 | 2.00 | 1.91±0.55 | 1.94±0.01 |
| Gd | 15.00 | 15.95±0.93 | 15.95±0.93 | 4.00 | 4.39±0.27 | 4.51±0.12 |
| Tb | 0.50 | 0.52±0.05 | 0.52±0.05 | 10.00 | 10.88±0.91 | 10.84±0.17 |
| Dy | 6.00 | 6.51±0.11 | 6.51±0.72 | 8.60 | 8.94±0.39 | 9.12±0.07 |

The ruggedness of the method was calculated by the comparison of the intra- and inter-day assay results for lanthanide ions undertaken by two analysts. The %R.S.D. values in the cited formulations performed in the same laboratory did not exceed 3.8 %, thus indicating the ruggedness of the method. Also, the robustness of the method was investigated under a variety of conditions such as small changes in the: pH of the eluent, flow rate, buffer composition and laboratory temperature. As seen in Table 5, the medium lanthanide ions recovery percentages were good under most conditions, not demonstrating any significant change when the critical parameters were modified.

Monazite [(Ln,Th)PO$_4$] and Xenotime [(Y,Ln)PO$_4$] are two important lanthanide ores and have large amounts of these elements. The first one is richer in earlier lanthanides and the second one is

richer in later lanthanides. Ion-exchange separation is not of real commercial importance for large-scale production, but historically it was the method by which fast high-purity separation of lanthanides first became feasible [56]. So, two solutions were prepared with the same ingredients of monazite and xenotime and diluted 1000 times to provide sample solutions (due to the amounts of samarium in monazite and gadolinium, and terbium in xenotime being so large, they were inevitably diluted 10 times more). The results obtained for medium lanthanide ions in monazite and xenotime samples under investigation are given in Table 6. For these determinations five replicate analyses were performed for each sample. The standard deviation of the whole procedure is also given in Table 6. From the results it can be seen that within the precision of both measuring procedures the concentration values of these ions determined by FFT-CCV and ICP-AES are in fair agreement with each other.

### 3.7. Comparison of the sensitivity of the proposed method and other previously reported methods

Table 7 compares the detection limit of the proposed method with UV-Vis spectrometry, spectrofluorimetry, RI, ICP-AES and potentiometric methods. The sensitivity of FFT-CCV method is better than most of them.

**Table 7.** Comparison between the detection limits of the proposed method with the other reported methods

| Separation Method | Detection Method | Detection Limit $(mg\ L^{-1})$ | Ref. |
|---|---|---|---|
| SPE-RP-Ion Pair-HPLC | UV, RI | 10 | 3 |
| IEC | Vis | ~ 10 | 4 |
| IEC | Vis | 5 | 5 |
| HPCIC | Vis | 4 | 6 |
| IEC | Spectrofluorimetry | > 50 | 7 |
| IEC | Spectrofluorimetry | > 50 | 8 |
| CE | UV | 0.24 – 0.47 | 9 |
| CE | UV | 0.53 – 0.96 | 10 |
| IEC | ICP-AES | 0.07 – 0.25 | 11 |
| RP-HPLC | UV-Vis | > 11 | 12 |
| RP-HPLC | Diod Array Detector | > 9 | 13 |
| CE | UV | 4.8 | 14 |
| IEC | Vis | 25 | 15 |
| - | Potentiometry | 0.47 | 28 |
| - | Potentiometry | 0.09 | 29 |
| - | Potentiometry | 0.10 | 30 |
| - | Potentiometry | 0.97 | 31 |
| - | Potentiometry | 0.75 | 33 |
| - | Potentiometry | 0.09 | 34 |
| - | Potentiometry | 0.09 | 35 |
| - | Potentiometry | 0.13 | 36 |
| IEC | FFT-CCV | 0.08 | This Work |

## 4. CONCLUSIONS

1. In this work the cation exchange separation and determination of Samarium, Europium, Gadolinium, Terbium and Dysprosium ions was achieved for the first time by coupling of ion exchange separation and Fast Fourier Transform Continuous Cyclic Voltammetry (FFT-CCV) in a flowing solution, thereby enabling direct detection.

2. α-hydroxyisobutyricacid (HIBA) has found to be a successful eluent. Lanthanide ions form complexes with HIBA, which lower the affinity of the lanthanide for the cation exchange resin. Lanthanide ions such as $Dy^{3+}$ form a stable complex with HIBA, spend more time in the eluent and elute first. Lanthanide ions such as $Sm^{3+}$ form a weaker complex with HIBA, spend relatively less time in eluent and elute later (the rate of transport being in the order $Dy^{3+}>Tb^{3+}>Gd^{3+}>Eu^{3+}>Sm^{3+}$).

3. From the results described in this study it can be concluded that good separation of these ions can be achieved using isocratic elution with 0.25 M of HIBA at pH 4.0. The best values for accumulation potential and accumulation time were -300 mV and 0.3 s respectively and 30 V s$^{-1}$ scan rate was necessary. The agreement between the results obtained by FFT-CCV and ICP-AES indicate the proposed method can lead to good accuracy.

**References**

1. M. R. Buchmeiser, *Rev. Anal. Chem.,* 20 (2001) 161.
2. T. Prasada Rao, V. M. Biju, *Crit. Rev. Anal. Chem.,* 30 (2000) 179.
3. M .R. Buchmeiser, G. Seeber and R. Tessadri, *Anal. Chem.,* 72 (2000) 2595.
4. C. H. Knight, R. M. Cassidy, B. M. Recoskie and L. W. Green, *Anal. Chem.,* 56 (1984) 474.
5. Y. Inoue, H. Kumagai and Y. Shimimura, *Anal. Chem.,* 68 (1996) 1517.
6. P .N. Nesterenko and P. N. Jones, *J. Chromatogr. A,* 804 (1998) 223.
7. Ş. Kutun and A. Akseli, *J. Chromatogr. A,* 847 (1999) 261.
8. Ş. Kutun and A. Akseli, *J. Chromatogr. A,* 874 (2000) 311.
9. N. Öztekin and F. B. Erim, *J. Chromatogr. A,* 895 (2000) 263.
10. N. Öztekin and F. B. Erim, *J. Chromatogr. A,* 924 (2001) 541.
11. E. H. Borai, M. A. Eid and H. F. Aly, *Anal. Bioanal. Chem.,* 372 (2002) 537.
12. E. Santoyo and S. P. Verma, *J. Chromatogr. A*, 997 (2003) 171.
13. N. M. Raut, P. G. Jaison and S. K. Aggarwal, *J. Chromatogr. A,* 1052 (2004) 131.
14. E. Santoyo, R. García, K. A. Galicia-Alanis, S. P. Verma, A. Aparicio and A. Santoyo-Castelazo, *J. Chromatogr. A,* 1149 (2007) 12.
15. A. Mazzucotelli, A. Dadone, R. Frache and F. Baffi, *Chromatographia,* 15 (1982) 697.
16. P. Henderson, *Rare Earth Element Geochemistry*, Elsevier, Amsterdam, 1984.
17. R. M. Cassidy, S. Elchuk, N. L. Elliot, L. W. Green, C. H. Knight and B. M. Recoskie, *Anal. Chem.,* 58 (1986) 1181.
18. D. J. Barkley, M. Blanchette, R. M. Cassidy and S. Elchuk, *Anal. Chem.,* 58 (1986) 2222.
19. S. Elchuk, K. I. Burns, R. M. Cassidy and C. A. Lucy, *J. Chromatogr.,* 558 (1991) 197.

20. E. A. Jones, H. S. Bezuidenhout and J. F. Van Staden, *J. Chromatogr.,* 537 (1991) 277.
21. R. Kuroda, T. Wada, G. Kishimoto and K. Oguma, *Chromatographia,* 32 (1991) 65.
22. L. E. Vera-Avila and E. Camacho, *J. Liq. Chromatogr.,* 15 (1992) 835.
23. R. G. Fernández and J. I. G. Alonso, *J. Chromatogr. A,* 1180 (2008) 59.
24. C. Nuryono, G. Huber and K. Kleboth, *Chromatographia,* 48 (1998) 407.
25. S .P. Verma, *Lanthan. Actin. Res.,* 3 (1991) 237.
26. K. Kawabata, Y. Kishi, O. Kawaguchi, Y. Watanabe and Y. Inoue, *Anal. Chem.,* 63 (1991) 2137.
27. B. A. Haley and G. P. Klinkhammer, *Mar. Chem.*, 82 (2003) 197.
28. F. Faridbod, M. R. Ganjali, R. Dinarvand, P. Norouzi and  S. Riahi, *Sensors*, 8 (2008) 1645.
29. M. R. Ganjali, M. R. Pourjavid, M. Rezapour and S. Haghgoo, *Sens. Actuators B*, 89 (2003) 21.
30. M. R. Ganjali, A. Ghesmi, M. Hosseini, M. R. Pourjavid, M. Rezapour, M. Shamsipur and M. Salavati-Niasari, *Sens. Actuators B*, 105 (2005) 334.
31. M. R. Ganjali, J. Ravanshad, M. Hosseini, M. Salavati-Niasari, M. R. Pourjavid and M. R. Baezzat, *Electroanalysis*, 16 (2004) 1771.
32. M. R. Ganjali, P. Norouzi, A. Daftari, F. Faridbod and M.Salavati-Niasari, *Sens. Actuators B*, 120 (2007) 673.
33. H. A. Zamani, G. Rajabzadeh, M. R. Ganjali and P. Norouzi, *Anal. Chim. Acta*, 598 (2007) 51.
34. M. R. Ganjali, Z. Memari, F. Faridbod, R. Dinarvand and P. Norouzi, *Electroanalysis*, 20 (2008) 2663.
35. H. A. Zamani, M. R. Ganjali, P. Norouzi, A. Tadjarodi and E. Shahsavani, *Mater. Sci. Eng. C*, 28 (2008) 1489.
36. P. T. Kissinger and W. R. Heineman, *Laboratory Techniques in Electroanalytical Chemistry*, Marcel Dekker, New York, 1984.
37. R. M. Wightman and D. O. Wipf, in: A. J. Bard (Ed.), *Electroanalytical Chemistry*, vol. 15, Marcel Dekker, New York, 1989.
38. M. Paeschke, F. Dietrich, A. Ulig and R. Hintsche, *Electroanalysis,* 8 (1996) 891.
39. G. Sreenivas, S. S. Ang, I. Fritsch, W. D. Brown, G. A. Gerhardt and D. Woodward, *J. Anal. Chem.,* 68 (1996) 1858.
40. A. S. Baranski, P. Norouzi and L. Nelsson,  *J. Proc. Electrochem. Soc.,* 96 (1996) 41.
41. CRC Handbook of Chemistry and Physics, 76th Edition, 1995.
42. P. Norouzi, M. R. Ganjali and P. Matloobi, *Electrochem. Commun.,* 7 (2005) 33.
43. P. Norouzi, G. R. Nabi Bidhendi, M. R. Ganjali, A. Sepehri and M. Ghorbani, *Microchim. Acta*, 152 (2005) 123.
44. M. R. Ganjali, P. Norouzi, M. Ghorbani and A. Sepehri, *Talanta*, 66 (2005) 1225.
45. P. Norouzi, M. Qomi, A. Nemati, M. R. Ganjali, *Int. J. Electrochem. Sci.,* 4 (2009) 1248-1261.
46. P. Norouzi, A. Nemati, N. Tajarod and M. R. Ganjali, *Int. J. Electrochem. Sci.,* 4 (2009) 1109-1115.
47. J. Lipkowski and L. Stolberg, *Adsorption of Molecules at Metal Electrodes*, VCH, New York, 1992.
48. J. O. M. Bockris, B. E. Conway and E. Yeager, *Comprehensive Treatise of Electrochemistry*, Plenum, New York, London, 1980.
49. P. Norouzi, S. Shirvani-Arani, P. Daneshgar and M. R. Ganjali, *Biosens. Bioelectron.,* 22 (2007) 1068.
50. P. Norouzi, M. R. Ganjali and P. Daneshgar, *Anal. Lett.,* 40 (2007) 547.
51. P. Norouzi, M. R. Ganjali, S. Labbafi and A. Mohammadi, *Anal. Lett.,* 40 (2007) 747.
52. P. Norouzi, M. R. Ganjali and P. Daneshgar, *J. Pharm. Toxicol. Method*, 55 (2007) 289.
53. A. E. Martell and R. M. Smith, *Critical StabilityConstants: Other Organic Ligands*, Vol. 3, Plenum, New York, 1977, p.28.
54. H. P. Fuping, P. R. Haddad, P. E. Jackson and J. Carnevale, *J. Chromatogr.,* 640 (1993) 187.

55. International Conference on Harmonization (ICH) Topic Q2 B: *Validation of Analytical Procedures: Methodology,* The European Agency for the Evaluation of Medicinal Products, Geneva, 1996.

56. *Lanthanide and Actinide Chemistry*, Simon Cotton, John Wieley & Sons, Ltd, 2006.